Title

Biogenic emissions of isoprenoids and NO in China and comparison to anthropogenic emissions

Permalink

https://escholarship.org/uc/item/741089j4

Journal

The Science of The Total Environment, 371(1-3)

ISSN

0048-9697

Authors

Tie, Xuexi
Li, Guohui
Ying, Zhuming
et al.

Publication Date

2006-12-01

DOI

10.1016/j.scitotenv.2006.06.025

Peer reviewed

Biogenic emissions of isoprenoids and NO in China and comparison to anthropogenic emissions

Xuexi Tie [a,*], Guohui Li [b], Zhuming Ying [c], Alex Guenther [a], Sasha Madronich [a]

[a] *National Center for Atmospheric Research, Boulder, CO, USA*
[b] *University of Texas A&M, College Station, TX, USA*
[c] *York University, Toronto, Canada*

Abstract

In this study, a regional dynamical model (WRF) is used to drive biogenic emission models to calculate high resolution (10×10 km) biogenic emissions of isoprene (C_5H_8), monoterpenes ($C_{10}H_{16}$), and nitric oxide (NO) in China. This high resolution biogenic inventory will be available for the community to study the effect of biogenic emissions on photochemical oxidants in China. The biogenic emissions are compared to anthropogenic emissions to gain insight on the potential impact of the biogenic emissions on tropospheric chemistry, especially ozone production in this region. The results show that the biogenic emissions in China exhibit strongly diurnal, seasonal, and spatial variations. The isoprenoid (including both isoprene and monoterpenes) emissions are closely correlated to tree density and strongly vary with season and local time. During winter (January), the biogenic isoprenoid emissions are the lowest, resulting from lower temperature and solar radiation, and highest in summer (July) due to higher temperature and solar radiation. The biogenic NO emissions are also higher during summer and lower during winter, but the magnitude of the seasonal variation is smaller than the emissions of isoprene and monoterpenes. The biogenic emissions of NO are widely spread out in the northern, eastern, and southern China regions, where high-density agricultural soil lands are located. Both biogenic NO and isoprenoid emissions are very small in western China. The calculated total biogenic emission budget is smaller than the total anthropogenic VOC emission budget in China. The biogenic isoprenoid and anthropogenic VOC emissions are 10.9 and 15.1 Tg year^{-1}, respectively. The total biogenic and anthropogenic emissions of NO are 5.9 and 11.5 Tg(NO) year^{-1}, respectively. The study shows that in central eastern China, the estimated biogenic emissions of isoprenoids are very small, and the anthropogenic emissions of VOCs are dominant in this region. However, in northeastern and southern China, there are relatively large biogenic emissions of isoprenoids, leading to an important impact on the ozone production in these regions. Furthermore, the emissions of isoprenoids are highest during summer and noontime, which correlates to the peak of ozone production period. For example, the ratio between summer and winter for the emissions of isoprenoids is about 15 in China. As a result, the biogenic emissions of isoprenoids are significantly larger than the anthropogenic emissions of VOCs in China during daytime in summer. Biogenic NO emissions are mostly produced by agricultural soils which co-exist with large populations and human activity. As a result, the biogenic emissions of NO are mostly overlapped with the anthropogenic emissions of NO, leading to the enhancement in NO concentrations in the high anthropogenic NO emission regions. Finally, the future emissions of isoprene and monoterpenes over China are estimated. The results show that the future biogenic emissions may increase significantly due to land cover changes in central eastern China, which could have a very important impact on ozone formation in this region. However, these estimates are highly uncertain and are presented as a potential scenario to show the importance of possible changes of biogenic emissions in China.
© 2006 Elsevier B.V. All rights reserved.

* Corresponding author. ACD/NCAR, P O BOX 3000, Boulder, CO 80303, USA. Tel.: +1 303 497 1470; fax: +1 303 497 1400.
  E-mail address: xxtie@ucar.edu (X. Tie).

1. Introduction

China is undergoing major economic changes, leading to heightened energy usage and a significant increase in pollutant emissions. For example, the energy consumption in China has increased more than 300% from 1973 to 2002 (IEA, 2004). The rapid increase in the energy usage will lead to a substantial increase in the anthropogenic emissions of VOCs (volatile organic compounds) and NO (nitrogen monoxide). Because VOCs and NO_x ($NO + NO_2$) are precursors of ozone formation, the rapid increase in the emissions of VOCs and NO_x can possibly result in enhancement of ozone production in China (Tie et al., 2006). The anthropogenic emissions over Asia, including China, have been estimated by Streets et al. (2003) and provide useful information for understanding the origin of air pollutants, especially for our modeling community. However, the emission inventory described by that study does not include biogenic emissions. There are a few measurements of biogenic VOC emissions, including grasslands in northern China (He et al., 2004), and tropical forest in southern China (Wang et al., 2005a, b; Baker et al., 2005; Geron et al., 2006). To fully understand the chemistry in China and to model the distributions of air pollutants, the biogenic emissions of VOCs and NO need to be estimated.

Biogenic emissions are important sources for VOCs. For example, in North America, biogenic VOC emissions are estimated to be more than seven times greater than anthropogenic VOC emissions [Guenther et al., 2000]. VOCs play a variety of important roles in the chemistry of the atmosphere, including enhancement in the production of peroxy (HO_2 and RO_2) radicals and organic aerosols. Biogenic VOCs react readily with available OH, which can control atmospheric reactivity, and further, impact the atmospheric lifetime of methane (CH_4), a greenhouse gas. In certain regions, it has been shown that biogenic VOCs play a key role in the reactions that form tropospheric ozone (O_3), which is both a pollutant and a greenhouse gas (e.g. Chameides et al., 1988; Fehsenfeld et al., 1992; Pierce and Novak, 1991). O_3 formation, however, is non-linear. The co-location of anthropogenic sources of oxides of nitrogen (NO_x) with biogenic sources of reactive VOC (particularly isoprene) can generate large amounts of tropospheric O_3, whereas biogenic sources located in areas without the presence of anthropogenic NO_x will not (Ryerson et al., 2001), and can in some instances reduce O_3 concentrations (e.g. Fiore et al., 2005). The biogenic emissions are not uniformly distributed. In some regions, biogenic emissions are a major component of the total VOC and NO emissions, while in other regions they are minor contributors. Furthermore, the short lifetimes (minutes to hours) of natural VOCs in the daytime troposphere result in large spatial and temporal variations in natural VOC mixing ratios (Guenther et al., 2000). To better understand air pollutants in China, a biogenic emission inventory with high spatial resolution is needed. Because isoprenoids (isoprene and monterpenes) are major contributors to total biogenic VOC emissions (Guenther et al., 2000), and have important impacts on atmospheric oxidants and aerosols (Lack et al., 2003; Wiedinmyer et al., 2006), isoprenoid emissions are considered as biogenic VOC emissions in this study.

In this paper, high horizontal resolution (10×10 km) biogenic emissions of isoprenoids (isoprene and monterpenes) and NO are estimated. First a method is described to estimate the biogenic emissions in China. Then the biogenic emissions are analyzed, including their budget, spatial distributions, and seasonal and diurnal variations. Furthermore, the biogenic emissions are compared to anthropogenic VOC and NO emissions to have some insight for the potential impact of biogenic emissions on ozone production in China. The paper is organized as follows: In Section 2, we will briefly describe the tools, including the dynamical WRF-Weather Forecast Model (WRF) and the biogenic models; in Section 3, the biogenic emissions are analyzed for China.

2. Method

In this section, the dynamical and biogenic emission models are described. According to the study by Guenther et al. (2000), there are four major factors in controlling biogenic emissions of isoprenoids and NO, which are foliar density, landscape emission potential, an emission activity factor to account for instantaneous light and temperature conditions and an emission activity factor to account for longer term controls over emission variations. With the above considerations, the fluxes of the biogenic emission can be calculated using the following equation,

$$ER_i = \Sigma_j[A_j \times AEF_{ij} \times ECF_i(PAR, \ T, \ Ts)] \qquad (1)$$

where ER_i is the emission rate of chemical species i, A_j is the area of vegetation class j, AEF_{ij} is the area-based emission factor of chemical species i for vegetation class j for standard conditions (normally at 303 K and 1000 μE (imol m^{-2} s^{-1}) of photosynthetically active radiation (PAR)), and ECF_i (PAR, T, Ts) is a unitless environmental correction factor representing the effects of temperature (T), soil temperature (Ts) and solar radiation (PAR) on emission. Note that AEF is based on the net emission into the atmosphere and so considers any reduction in emission

Table 1

The categories of USGS land cover, and the referenced emission rates for isoprene, monoterpenes ($\mu gC\ m^{-2}\ h^{-1}$), and nitric oxide at 303 K and 1000 μE (μmol photons $m^{-2}\ s^{-1}$) of photosynthetically active radiation (PAR)

	ISO	MTER	NO	Ref
1 Urban and built-up land	0 (0)	0 (0)	0	A1
2 Dryland cropland and pasture	8 (0)	20 (0)	9	S+R
3 Irrigated cropland and pasture	8 (0)	20 (0)	9	S+R
4 Mix. dry/irrg. cropland and pasture	8 (0)	20 (0)	9	S+R
5 Cropland/grassland mosaic	4 (0)	20 (10)	4.9	A2
6 Cropland/woodland mosaic	2204 (0)	202 (0)	4.5	A2
7 Grassland	0 (0)	20 (20)	0.9	S+R
8 Shrubland	0 (0)	20 (20)	0.1	A2
9 Mixed shrubland/grassland	0 (0)	20 (20)	0.1	A2
10 Savanna	0 (0)	0 (0)	0	Z88
11 Deciduous broadleaf forest	4400 (0)	385 (0)	0.1	G94
12 Deciduous needleleaf forest	780 (0)	1380 (0)	0.1	G94
13 Evergreen broadleaf forest	4400 (4400)	385 (385)	0.1	G94
14 Evergreen needleleaf forest	780 (780)	1380 (1380)	0.1	G94
15 Mixed Forest	5775 (2887)	1001 (500)	0.1	G94
16 Water Bodies	0 (0)	0 (0)	0	A1
17 Herbaceous wetland	0 (0)	0 (0)	0	A1
18 Wooded wetland	5775 (2887)	1001 (500)	0.1	A3
19 Barren or sparsely vegetated	0 (0)	0 (0)	0	A1
20 Herbaceous tundra	70 (0)	0 (0)	0	K94
21 Wooded tundra	70 (0)	0 (0)	0	K94
22 Mixed tundra	70 (0)	0 (0)	0	K94
23 Bare ground tundra	0 (0)	0 (0)	0	A1
24 Snow or ice	0 (0)	0 (0)	0	A1
25 No data	0 (0)	0 (0)	0	A1

The numbers are for averaged values from April to September, and the numbers in parentheses are for the values from October to March ("base" case).

S+R: Schoenemeyer et al. (1997).

Z88: Zimmerman et al. (1988).

G94: Guenther et al. (1994).

K94: Klinger et al. (1994).

A1: Assumed to be zero.

A2: Obtained from S+R's cropland and grassland values (0.5cropland+0.5grassland).

A3: Assumed to be the same as the mixed forest values.

due to losses by canopy uptake. In the model, temperature, soil temperature, and solar radiation at each horizontal grid point are calculated at each time step. These dynamical parameters are used in Eq. (1) to calculate the emission rates. Each component of the equation used in this study will be described in the following sections.

2.1. Dynamical inputs (PAR, T, Ts) and land covers

Accurate prediction of biogenic emissions relies on accurate characterizations of land cover, surface temperature, soil temperature, and photosynthetically active radiation (visible solar radiation). In this study, dynamical parameters (surface temperatures, soil temperatures, and solar radiation) are calculated using a state of the art regional dynamical/transport model (the Weather Research Forecasting (WRF) model) developed at NCAR and NOAA in collaboration with other institutions. The model includes calculation of dynamical parameters

(winds, temperature, boundary layer, clouds etc). The horizontal resolution of the model is flexible, ranging from a few km to several hundred km. A detailed description of the model can be found at the WRF web-site at http://www.wrf-model.org/index.php.

Detailed land use data (1×1 km horizontal resolution) from USGS (US Geological Survey) are included in the emission calculation in the WRF model. The categories of land use are listed in Table 1. High biogenic isoprenoid emission potentials are confined to roughly 1/3 of woody tree species and are much less common in shrubs and grasses (e.g. Guenther et al., 1994). To illustrate the vegetation distributions in China, we show in Fig. 1 shows the estimated vegetation distribution in China (excluding western China where there is almost no vegetation). Large forest area (mixed needleleaf and broadleaf forests) in China are located in northeastern, central eastern and southern China. There is a small tropical rainforest area in the Yunnan province
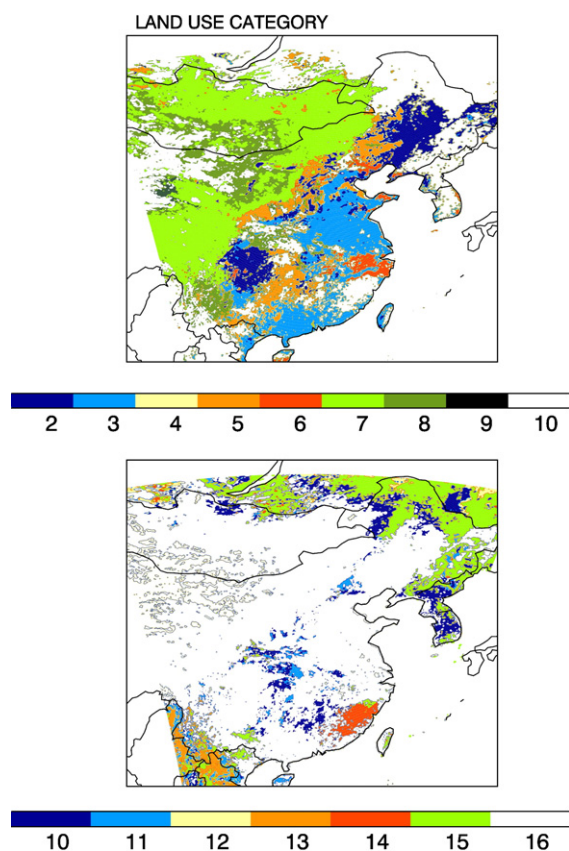
LAND USE CATEGORY

Fig. 1. The USGS landcover map used in the model.

(in southern China). Large areas of agricultural soil lands are located in central eastern China. In western China, there is very little vegetation canopy cover or agricultural lands. A description of the landcover type index and the corresponding standard emission factors (AEF in Eq. (1)) for isoprene, monoterpenes, and NO used for the model calculation are also shown in Table 1. Note that the seasonal variation of foliar biomass of vegetations is considered and indicated in Table 1.

In this study, the WRF model calculates temperature and solar radiation every 60 s. The calculation of biogenic fluxes is saved in each hour, and then the monthly averaged fluxes are calculated in January, April, July, and October to represent winter, spring, summer, and fall conditions, respectively. The horizontal resolution of the model is 10×10 km centered in central China.

2.2. The temperature and light dependence

To calculate the environmental correction factor (ECF in Eq. (1)) representing the effects of air temperature (T), soil temperature (Ts) and solar radiation (PAR) on emissions, the algorithms of Guenther et al. (1993) are used to provide the emission fluxes of isoprene and monoterpenes under different temperature and solar radiation conditions. The study by Guenther et al. (1993) shows that the emissions of isoprene are strongly related to both temperature and solar radiation, but the emissions of monoterpenes are considered to be solely temperature dependent. As a result, the magnitude of the seasonal and diurnal variations of the emissions of isoprene is generally larger than for the emissions of monoterpenes.

2.2.1. Isoprene

According to Guenther et al. (1993), the emission correction factor for isoprene emission (ECF_I) is described by the following equation:

$$ECF_I = C_L C_T \tag{2}$$

where C_L is the factor describing the response of emission rate to solar radiation and is defined as follows:

$$C_L = \alpha C_{L1} L / [\sqrt{(1 + \alpha^2 L^2)}] \tag{3}$$

where $\alpha (=0.0027)$ and $C_{L1} (=1.066)$ are empirical coefficients. L is photosynthetically active radiation (PAR).

The response to temperature, C_T, is described by the equation

$$C_T = \exp[C_{T1}(T-Ts)/(RTsT)]/\{1 + \exp[C_{T2}(T-T_M)/(RTsT)]\} \tag{4}$$

where R is a constant ($=8.314$ J K^{-1} mol^{-1}). and C_{T1} ($=95,000$ J mol^{-1}), and $C_{T2}(=230,000$ J mol^{-1}) are empirical coefficients. T, Ts, and T_M (314 K) are air temperature, soil temperature, and reference temperature, respectively.

2.2.2. Monoterpenes

The emission correction factor for monoterpene emissions (ECF_M) can in some cases be simulated by Eq. (2) and in other cases it follows the behavior described by Guenther et al. (1993) as:

$$ECF_M = \exp(\beta(T-Ta)) \tag{5}$$

where ECF_M is the temperature correction factor for monoterpene emission rate at temperature T (K), Ta is a standard temperature (here 303 K), and $\beta (=0.09$ K^{-1}) is an empirical coefficient. Baker et al. (2005) have recently demonstrated that monoterpene emissions from subtropical Chinese vegetation can be light-dependent but it is not known if this behavior is widespread in China. We have used Eq. (5) to simulate monoterpene

emissions but recognize that additional measurements are needed to determine if a significant fraction of monoterpene emissions is light dependent.

2.2.3. Nitrogenmonoxide

Emissions of NO from soils might make an important contribution to NO_x levels in remote areas (Skiba et al., 1992; Simpson et al., 1990; Stocker et al., 1993; Williams and Fehsenfeld, 1991). Based upon the work of Pierce and Novak (1991), the correction factor of NO is dependent upon the soil temperature, and the following formula is used to estimate the correction factor for NO biogenic flux:

$$ECF_{NO} = \exp(0.071 Ts) \tag{6}$$

where ECF_{NO} is the correction factor for NO emission, and Ts is soil temperature (°C). Schindlbacher et al. (2004) suggested that the biogenic NO emissions change with soil moisture. In this study, Eq. (6) is used to simulate NO

emissions but additional measurements are needed to determine if a significant fraction of NO emissions is moisture dependent.

3. Calculated emission fluxes

3.1. Horizontal, seasonal, and diurnal distributions

Fig. 2A shows the calculated averaged isoprene emission fluxes in China for January, April, July, and October of 2004 respectively. In the following discussion, the reported fluxes are estimated for the total flux from each 10×10 km grid cell, and the calculated results in January, April, July, and October approximately represent winter, spring, summer, and fall conditions. Because of the complicated land coverage (desert, grassland, croplands, wood forest, etc.) and the wide range of the latitudes (from 15°N to 60°N) in China, there are considerable spatial and temporal variations in the isoprene emission
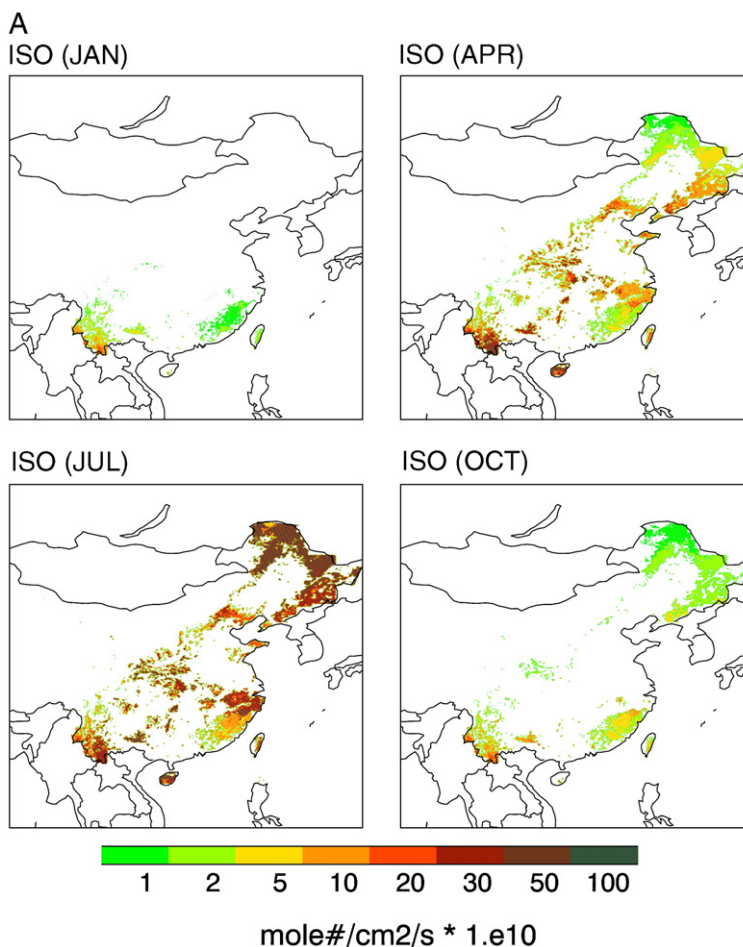

Fig. 2. (A) Calculated biogenic emissions of isoprene (mol# cm^{-2} $s^{-1} \times 10^{10}$) in January, April, July, and October, respectively. (B) Same as (A), except for monoterpenes. (C) Same as (A), except for NO.
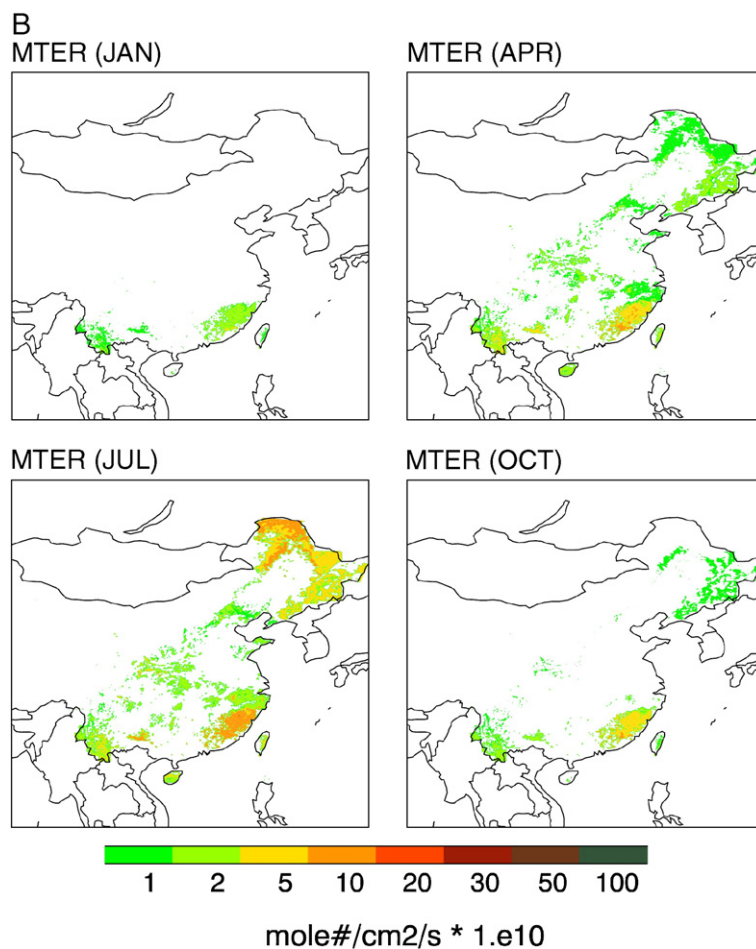
Fig. 2 (*continued*).

fluxes (see Fig. 2A). During January, the isoprene emissions are the highest in southern China where evergreen and deciduous forests have the highest density such as in Yunnan and Fujan (in southeastern China) Provinces. Note that during January, deciduous forests play important roles only in southern part of China. During April, due to the increase in both temperature and solar radiation, the isoprene emissions increase substantially throughout China. There are relatively high isoprene emissions in northeastern China where evergreen and deciduous forest density is very high in this high latitude region (latitude > 50°N). As temperature and solar radiation increases in July, the isoprene emissions reach the maximum values of the year, especially in the regions where evergreen and deciduous forest density is high, e.g. in southern and northeastern China. During October, the isoprene emissions start to decrease. The calculated total isoprene emissions are 0.18, 2.00, 5.05, and 0.47 Tg in winter, spring, summer, and fall, respectively, with an annual averaged value of 7.7 Tg year^{-1} in China. The

ratio of biogenic isoprene emissions between summer and winter is very large (about 27). This strong seasonal variation is due to the fact that the isoprene emissions are strongly dependent on the variability of both temperature and solar radiation. Table 2 shows that the estimated annual isoprene emissions fall between the values reported by Guenther et al. (1995) and Klinger et al. (2002).

The spatial distribution of monoterpene emissions is similar to the isoprene emissions (see Fig. 2B), except that the magnitude of the emissions are smaller than the isoprene emissions. The calculated monoterpene emissions are 0.16, 0.81, 1.78, and 0.41 Tg in winter, spring, summer, and fall respectively, with an annual averaged value of 3.16 Tg year^{-1} (see Table 2). The annual value is similar to the estimates of Guenther et al. (1995) and Klinger et al. (2002) shown in Table 2. The annual mean monoterpene emission is about a factor of 2 times smaller than the annual mean isoprene emission in China. One reason to explain the smaller monoterpene flux is that the
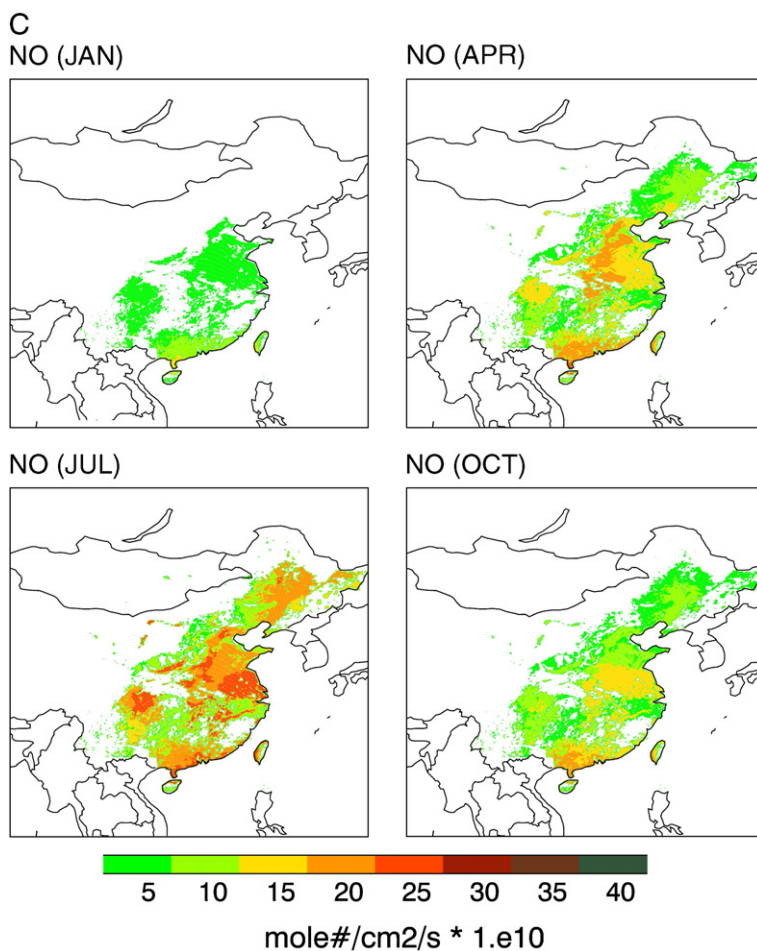
Fig. 2 (*continued*).

monoterpene emission factor from broadleaf forest and mixed forest is much smaller than the isoprene emission factor (see Table 1). The ratio of biogenic emissions of monoterpenes between summer and winter is about 11, which is also smaller than the ratio of isoprene. This is due both to a lack of light dependence for monoterpene emissions and also because isoprene emission has a stronger temperature dependence.

The spatial distributions of biogenic emissions of NO are different from the biogenic isoprenoid emissions (see Fig. 2C). The biogenic emissions of NO are high in agricultural soil lands where fertilizer containing nitrogen is applied to the land and later released to the air in the form of NO. The geographic location of the high biogenic NO emissions is in northern, eastern, and southern China, co-located with high density agricultural soils. The calculated NO emissions are 0.68, 1.64, 2.25, and 1.40 in winter, spring, summer, and fall respectively, with an annual emission of 5.97 Tg year^{-1} (see Table 2). The ratio of biogenic NO emissions

between summer and winter is 3.3, which is much smaller than the ratio of isoprene and monoterpene emissions. As shown in Eq. (6), the magnitude of biogenic NO emissions is dependent on soil temperature, and the seasonal variation of soil temperature is normally smaller than that of the air temperature. In addition, the increase in NO per degree K soil

Table 2
Calculated averaged biogenic emission budgets (Tg per season or per year)

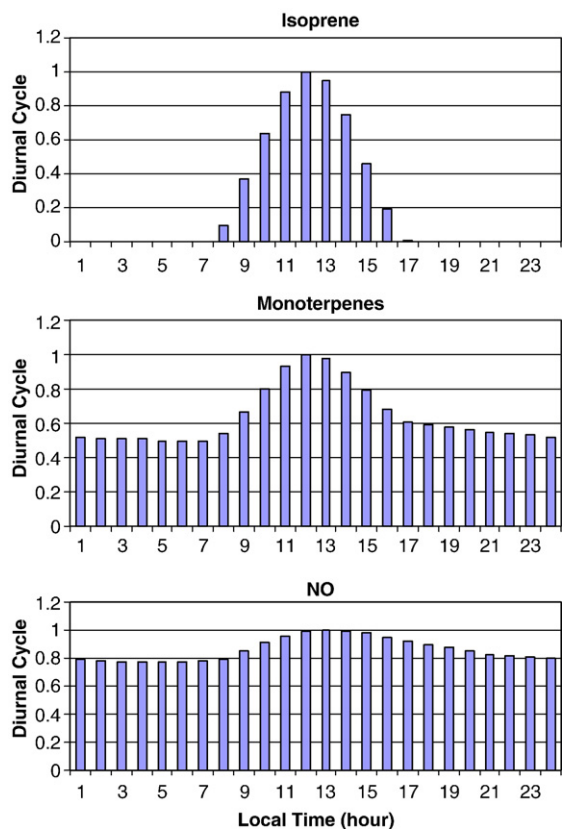|	Isoprene	Monoterpenes	NO	Reference
Winter	0.18	0.16	0.68	This study
Spring	2.00	0.81	1.64	This study
Summer	5.05	1.78	2.25	This study
Fall	0.47	0.41	1.40	This study
Annual	7.7	3.16	5.97	This study
Annual	4.1	3.5	–	Klinger et al. (2002)
Annual	15	4.3	–	Guenther et al. (1995)

Fig. 3. Calculated diurnal cycle of biogenic emissions of isoprene (upper panel), monoterpenes (middle panel), and NO (lower panel). The values of the diurnal cycle are the ratio of the maximum value and the local time values.

temperature is less than the increase in biogenic isoprenoids per degree K air temperature.

As well as seasonal variability, there is also a strong diurnal variation in biogenic emissions. Fig. 3 shows diurnal variation of biogenic emissions of isoprene, monoterpenes, and NO. In general, biogenic emissions are highest at or shortly after noon and lowest at night. The isoprene emissions have the highest diurnal variability. During noontime, the isoprene emissions reach a maximum, and quickly reduce in the afternoon. During the night, the isoprene emissions are zero, as a result of the absence of solar radiation. As discussed in the following sections, this strong diurnal cycle has an important impact on ozone concentrations in China. Because the diurnal variability of the monoterpene emissions is only dependent on temperature in this study, the magnitude of the diurnal variability of monoterpene emissions is smaller than the emissions of isoprene. Unlike isoprene emission, the emissions of monoterpenes are not zero during the night. However, the emissions are much smaller during the night (with
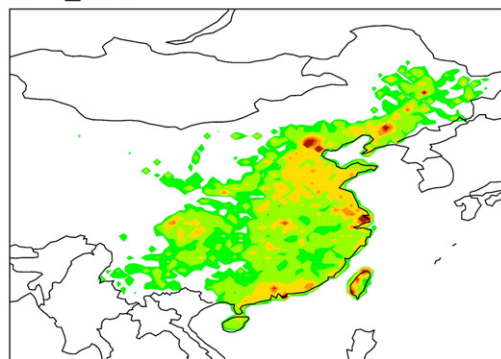
lower temperature) than the emissions during daytime (with higher temperatures). The ratio of the emissions between nighttime and noontime is approximately 0.5 (see middle panel of Fig. 3).

The biogenic emission of NO is dependent on soil temperature (Pierce and Novak, 1991), resulting in a weak diurnal variability. The ratio of the emissions between nighttime and noontime is approximately 0.8 (see lower panel of Fig. 3).

3.2. Comparison to anthropogenic emissions

The analysis by Tie et al. (2006) shows that the relatively low anthropogenic emissions of VOCs limit ozone production in eastern China during summer. As a result, the biogenic emissions of VOCs and NO can play important roles in controlling ozone concentrations in China. Thus, it is important to compare the biogenic
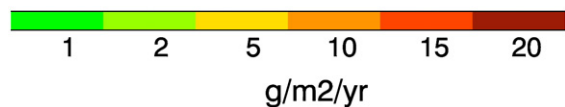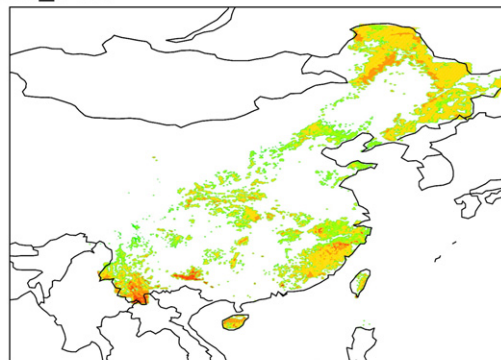

Fig. 4. Calculated annually averaged anthropogenic (upper panel, Streets et al., 2003) and biogenic emissions (lower panel) of VOCs (g m^{-2} year^{-1}).
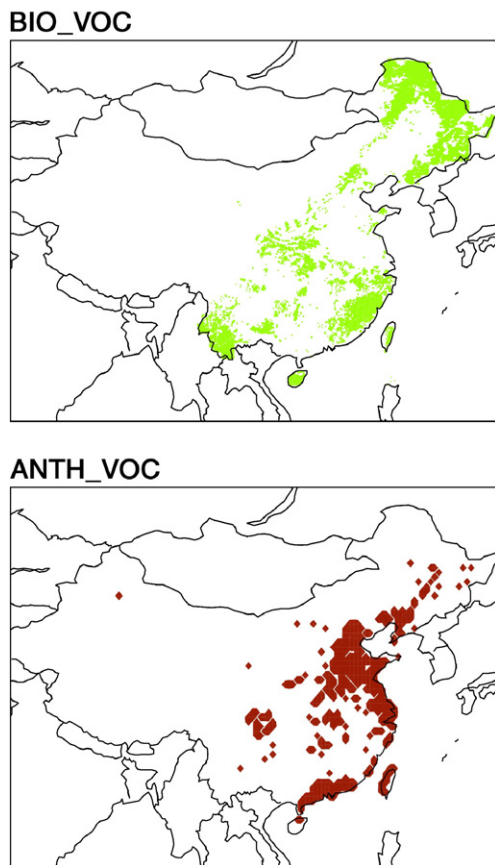
BIO_VOC

ANTH_VOC

Fig. 5. The comparison of the spatial distributions of anthropogenic emissions of VOCs and biogenic emissions of isoprenoids. The areas in green represent locations where biogenic emissions of isoprenoids are greater than 5 g m^{-2} year^{-1}, and the areas in brown represent locations where anthropogenic emissions of VOCs are greater than 5 g m^{-2} year^{-1}.

emissions to anthropogenic emissions to have some insight into the impact of biogenic emissions on tropospheric chemistry, especially ozone concentrations, in this region.

Fig. 4 shows both the annually averaged anthropogenic VOC and biogenic isoprenoid emissions in China. The anthropogenic VOC emissions are obtained from the study of Streets et al. (2003). The results show that the highest anthropogenic VOC emissions are mostly along the east coast of China, where there are high industrial activities and high-density population. There is also a clear indication that the VOC emissions have highest values in mega city areas, e.g. in Beijing, Shanghai, and Guangzhou. By contrast, the biogenic emissions of isoprenoids have highest values in high-density forest areas, such as northeastern and southern China. The calculated annual averaged anthropogenic emissions of VOCs are 15.1 Tg year^{-1}, and the biogenic

emissions of isoprenoids are 10.9 Tg year^{-1}. The total annual amount of biogenic emissions of isoprenoids is about 30% smaller than the anthropogenic emissions of VOCs. However, it is misleading to conclude that the smaller total annual biogenic emissions of isoprenoid play a less important role than the anthropogenic emissions, because the significant spatial and temporal variability of biogenic emissions of isoprenoids (see Figs. 2A,B and 3) could lead to important impacts on ozone concentrations in particular locations, where the biogenic emissions are much higher than the anthropogenic emissions. In addition to the different distributions, the relationship between ozone and VOCs is very complicated and non-linear (Sillman, 1995). The co-location of anthropogenic sources of oxides of nitrogen (NO$_x$) with biogenic sources of reactive isoprenoids (particularly isoprene) can generate large amounts of tropospheric O$_3$, whereas biogenic sources located in areas without the presence of anthropogenic NO$_x$ will not (Ryerson et al., 2001) and can, in some instances, reduce O$_3$ concentrations. As a result, the impact of biogenic emissions on the ozone is different when the biogenic emissions of isoprenoids are co-located with the anthropogenic emissions of VOC compared to when they are not. In order to address this issue, Fig. 5 shows the location of areas with significant (>5 g m^{-2} year^{-1}) anthropogenic and biogenic isoprenoid emissions. It shows that the areas with significant biogenic emissions of isoprenoids have almost no overlap with those with significant anthropogenic emissions of VOCs, indicating that the biogenic emissions of isoprenoids play an important role for the enhancement in ozone production in remote regions. However, in most industrial and populated areas, the enhancement of ozone production by biogenic emissions of isoprenoids is small.
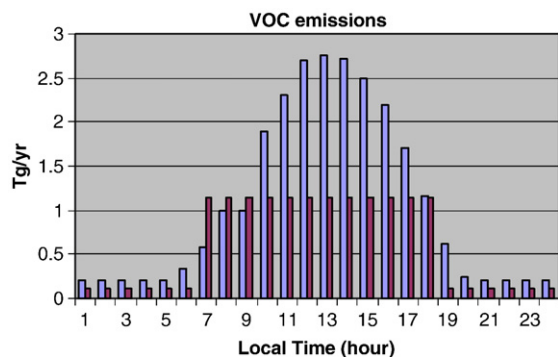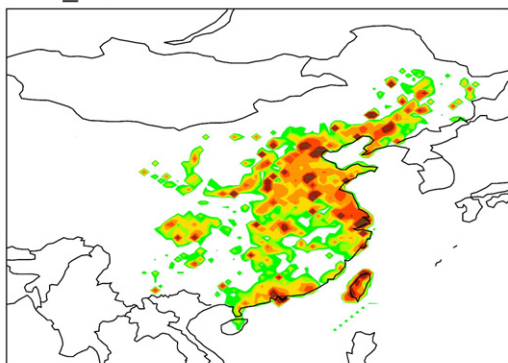

Fig. 6. Calculated diurnal cycle of biogenic isoprenoids in summer (light bars), and anthropogenic emissions of VOCs (dark bars) over China.
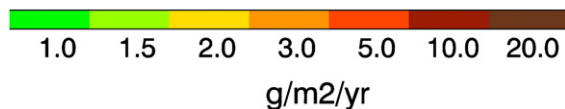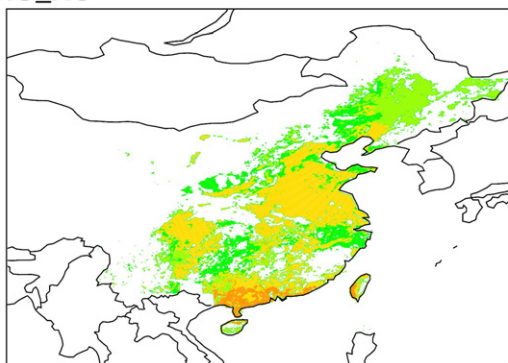
Fig. 7. Same as Fig. 4 except for NO.

In addition to the strong spatial distribution, the strong temporal variability of biogenic emissions is another important factor in determining the importance of its role in ozone production. In polluted areas, ozone production is highest during noontime in the summer, resulting from the strong photochemical activities at that time (Zhang et al., 2004; Tie et al., 2006). This also corresponds with the seasonal and diurnal cycles of isoprene and monoterpene emissions. Fig. 6 shows the diurnal variability of total annual biogenic and anthropogenic emissions of VOCs in China in summer. In the study of Streets et al. (2003), there is no information regarding the seasonal and diurnal variation of anthropogenic emissions of VOCs. In order to compare the biogenic emissions to anthropogenic emissions of VOCs, we assume that (1) the seasonal variation of anthropogenic emissions of VOCs is constant, and (2) the daytime anthropogenic emissions of VOCs are 10 times higher than nighttime emissions. With these assumptions, we see from Fig. 6 that the biogenic emissions

of isoprenoids are significantly larger than the anthropogenic emissions during daytime in the summer. During noontime when the rate of ozone production is at a maximum, the biogenic emissions of isoprenoids are more than 2 times higher than the anthropogenic emissions. This result demonstrates that even though the annual total of biogenic emissions of isoprenoids is smaller than the annual total of the anthropogenic emissions in China, the biogenic emissions could play an important role in controlling ozone production due to large spatial and temporal variability of biogenic emissions.

Fig. 7 shows the annual averaged anthropogenic and biogenic NO emissions over China. Similar to the anthropogenic VOC emissions, the anthropogenic NO emissions are also mostly located along the east coast of China. The calculated annual averaged total anthropogenic
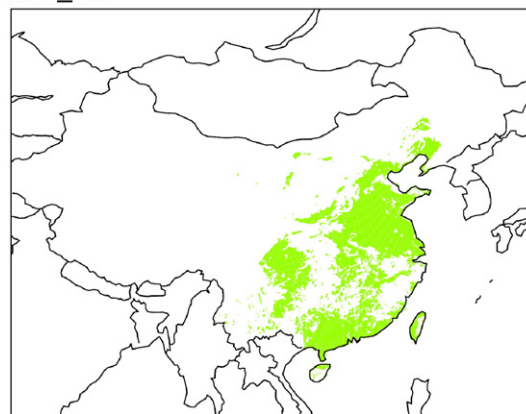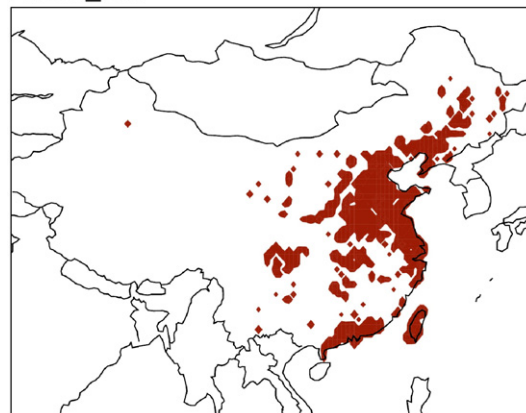

Fig. 8. The comparison of the spatial distributions of anthropogenic and biogenic emissions of NO. The areas in green represent locations where biogenic NO emissions are greater than $2 \text{ g m}^{-2} \text{ year}^{-1}$, and the areas in brown represent locations where anthropogenic NO emissions are greater than $2 \text{ g m}^{-2} \text{ year}^{-1}$.

emission of NO is 11.5 Tg year^{-1}, and the total biogenic emission is 5.9 Tg year^{-1}. The ratio of biogenic emissions to anthropogenic emissions is about 0.5. The highest biogenic NO emissions are located in southern China, where the high soil temperature and highly populated agricultural areas with associated activities produce the highest biogenic emissions of NO. In central eastern China, the biogenic NO emissions are high, while the biogenic isoprenoid emissions are low, resulting from high-density agriculture and little forest area. The satellite measurements (GOME, Global Ozone Monitoring Experiment) show that in central eastern China, there are very high NO$_x$ concentrations, and the high NO$_x$ concentrations play important roles in regulating ozone concentrations (producing ozone in the summer and destroying ozone in the winter) (Zhao et al., 2006). Fig. 8 shows the spatial locations of anthropogenic and biogenic NO emissions and the overlapped areas of both emissions. It shows that in central eastern China, the biogenic NO emissions are largely overlapped with the anthropogenic emissions of

NO. As a result, the biogenic NO emissions enhance the total annual NO emission in central eastern China, implying that biogenic NO emissions could be important to ozone regulation in this region. In general, the biogenic emissions of NO are largely overlapped with the anthropogenic emissions of NO, while the biogenic emissions of isoprenoids are not overlapped with the anthropogenic emissions of VOCs in China.

3.3. Estimate of uncertainty and future biogenic emissions over China

There is uncertainty related to the estimation of emission factors listed in Table 1. Wang et al. (2005a,b) report that various estimates of emission factors differ by ∼ 35% and that uncertainties in landcover distributions and associated emission factors are a major component of the total uncertainties associated with biogenic emissions. In order to assess the effect of uncertainty of emission factors on the biogenic emission inventory, the emission factors are compared with those developed for China by Wang et al. (2005a,b) and He et al. (2004) (see Table 3). This "new" estimate of biogenic emission is compared to the "base" estimate inventory of isoprenoids. Fig. 9A shows the large difference of isoprenoid emissions between "new" and "base" occurring in central China, with a maximum increase of 20×10^{10} mol# cm^{-2} s^{-1} for isoprene emission. The estimated emissions of isoprene are 2.2 Tg and 1.7 Tg and the estimated emissions of monoterpenes are 0.8 Tg and 0.6 Tg in July using "new" and "base" emission factors, respectively. The "new" estimation of isoprene and monoterpenes emissions is about 29% and 33% higher than the "base" estimation, respectively, which are within the uncertainty range of the ∼ 35% as suggested by Wang et al. (2005a,b).

Another important issue regarding the estimated biogenic emission is that the vegetation cover in Chinese landscapes has changed dramatically over the past centuries and is expected to continue to change considerably in the next 20 to 50 years. The past changes are primarily associated with the replacement of forests by croplands and urbanization in Eastern China. This is expected to have resulted in a large decrease in biogenic isoprenoid emissions and an increase in biogenic NO emissions. The current trend in China is an increase in forest plantations in the countryside, and vegetation covered areas within urban zones and the planted trees tend to have very high isoprenoid emission rates (Klinger et al., 2002; Geron et al., 2006). The result is some landscapes with emission rates that are much higher than the natural forest landscape (Klinger et al., 2002). Geron et al. (2006) describe the substantial landcover changes that are expected to occur

Table 3

Categories of USGS land cover, and the emission rates for isoprene, monoterpenes (Cμg/m^2/h), and nitric oxide at 303 K and 1000 μE (μmol photons m^{-2} s^{-1}) of photosynthetically active radiation (PAR)

	ISO	MTER	NO
1 Urban and built-up land	8 (800)	8 (300)	0
2 Dryland cropland and pasture	8 (1200)	20 (200)	9
3 Irrigated cropland and pasture	8 (1200)	20 (200)	9
4 Mix. dry/irrg. cropland and pasture	8 (1200)	20 (200)	9
5 Cropland/grassland mosaic	4 (600)	20 (100)	4.9
6 Cropland/woodland mosaic	2200 (2400)	200 (400)	4.5
7 Grassland	20 (20)	20 (20)	0.9
8 Shrubland	1200 (1200)	20 (20)	0.1
9 Mixed shrubland/grassland	500 (500)	20 (20)	0.1
10 Savanna	1100 (1100)	200 (200)	0
11 Deciduous broadleaf forest	5000 (5000)	400 (400)	0.1
12 Deciduous needleleaf forest	200 (200)	1400 (1400)	0.1
13 Evergreen broadleaf forest	5000 (5000)	400 (400)	0.1
14 Evergreen needleleaf forest	800 (800)	1400 (1400)	0.1
15 Mixed forest	2500 (2500)	1000 (900)	0.1
16 Water bodies	0 (0)	0 (0)	0
17 Herbaceous wetland	70 (70)	0 (20)	0
18 Wooded wetland	4000 (4000)	1000 (900)	0.1
19 Barren or sparsely vegetated	0 (0)	0 (0)	0
20 Herbaceous tundra	70 (70)	20 (20)	0
21 Wooded tundra	130 (130)	30 (30)	0
22 Mixed tundra	100 (100)	30 (30)	0
23 Bare ground tundra	0 (0)	0 (0)	0
24 Snow or ice	0 (0)	0 (0)	0
25 No data	0 (0)	0 (0)	0

The emission factors were derived from the biogenic emission inventory described by Wang et al. (2005b) ("new" case). The numbers in parentheses are the assumed biogenic emission rates in the future due to predicted land-cover changes in China.
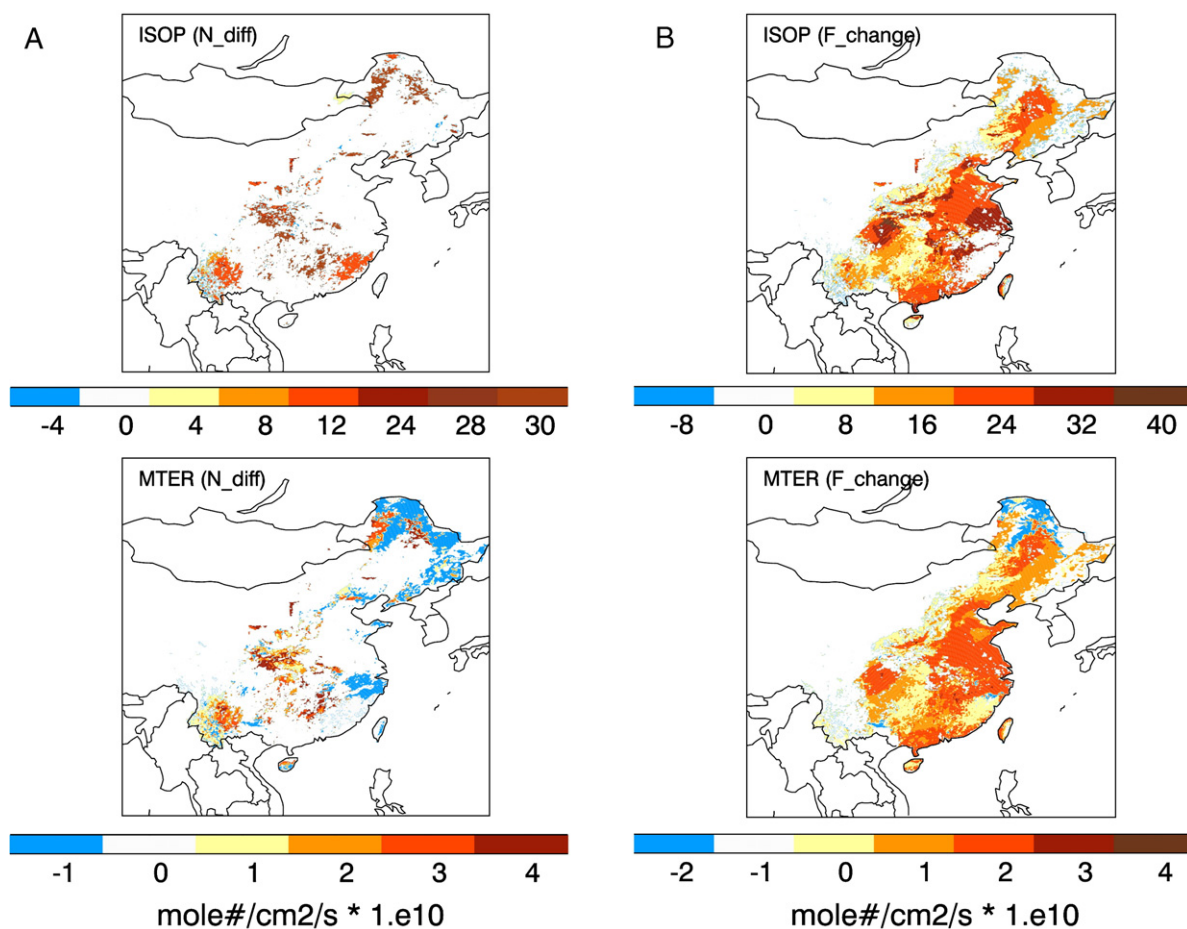
Fig. 9. (A) Calculated differences in emissions of isoprenoids (mol# cm^{-2} s^{-1} $\times$ 10^{10}) between "new" (Table 3) and "base" (Table 1) isoprene and monoterpene emission data base in July. (B) Calculated differences between estimated future and current isoprene and monoterpene emissions (mol# cm^{-2} s^{-1} $\times$ 10^{10}) in July. The differences are based on assumed land cover changes shown in Table 3.

in China in the next few decades. It is important to estimate future biogenic emissions when developing pollution mitigation strategies because assumptions about biogenic emissions could potentially change the optimal control strategy. This is especially important in China where the O$_3$ production in some areas is currently VOC limited, but may not be if biogenic isoprenoid emissions increase substantially. A simple scheme is applied to estimate potential future biogenic emissions in China (Table 3). We have adjusted the emission factors assigned to each landcover type to reflect the expected change in emissions associated with the landcover changes summarized by Geron et al. (2006). As we evaluate potential future chemistry scenarios for the purpose of better understanding the drivers and impacts and designing pollution control strategies, it is important to consider the potential changes and impacts of biogenic emissions. We understand that these estimates of future emissions are highly uncertain, but present these potential emission

scenarios to show the importance of possible changes of biogenic emission in China.

Fig. 9B shows the estimated changes between current and future emissions of isoprene and monoterpenes for July. It indicates that both the isoprene and monoterpene emissions increase significantly, especially in central eastern China where large croplands are currently located in these regions with a maximum increase of 40×10^{10} mol cm^{-2} s^{-1} for isoprene emissions. The monthly flux of isoprene emission is about 3.3 Tg in July which is a 94% increase compared to the current emission estimates. The monthly flux of monoterpene emissions is about 0.9 Tg, which is a 50 % increase compared to the current emission. More importantly, because most increases in biogenic emissions are located in central eastern China where ozone formation is strongly VOC limited (Tie et al., 2006), the large increases in biogenic VOC emissions could lead to significant increases in ozone chemical production in this region.

4. Summary

The study shows that the annual averaged total annual biogenic emissions of isoprenoids (isoprene and monoterpenes) are 10.9 Tg year^{-1} and the biogenic emissions of NO are 5.9 Tg year^{-1} with strong spatial and temporal variability. In winter (January), the biogenic emissions are lowest as a result of lower temperature and sunlight, and highest in summer (July) due to the increase in temperature and sunlight. The biogenic emissions of NO are also high during summer, and low during winter, with a smaller seasonal variation compared to the emissions of isoprene and monoterpenes. Because the biogenic isoprene emissions depend upon solar radiation, the isoprene emissions have the greatest diurnal variability with highest emission during noontime, and lowest during night. The magnitude of the diurnal variability of emissions of monoterpenes is smaller than that of emissions of isoprene. Compared to anthropogenic emissions, the biogenic emissions of isoprenoid and NO are smaller than anthropogenic emissions of VOCs and NO by 30% and 50%, respectively. The biogenic emissions of NO are largely co-located with the anthropogenic emissions of NO in China, while the biogenic emissions of isoprenoids are not overlapped with the anthropogenic emissions of VOCs. Although total annual biogenic emissions (10.9 Tg year^{-1}) of isoprenoids are smaller than the anthropogenic emissions (15.1 Tg year^{-1}) in China, the strong seasonal and diurnal cycles of biogenic emission could have important impacts on ozone concentrations. For example, during daytime in summer when the rate of ozone production is at a maximum, the biogenic emissions of isoprenoids are significantly larger than the anthropogenic emissions. Emissions estimated using alternative emission factors differed from the base study by less than 35% and were within the range suggested reported by previous studies. Finally, the future emissions of isoprene and monoterpenes are estimated based on future changes in land cover. The results show that the estimated future biogenic emissions may significantly increases in central eastern China, which could have a significant impact on ozone formation in this region. These estimates of potential emission scenarios are highly uncertain, but the results are presented to show the importance of possible changes in biogenic emissions in China.

Acknowledgement

References

Baker BC, Johnson C, Zhong-Tao JH, Bai L, Qing-Jum Y, Wang A, et al. Wet and dry season ecosystem level fluxes of isoprene and monoterpenes from a southeast Asian secondary forest and rubber tree plantation. Atmos Environ 2005;39:81-390.

Chameides W, Lindsay R, Richardson J, Kiang C. The role of biogenic hydrocarbons in urban photo-chemical smog: Atlanta as a case study. Science 1988;241:1473–5.

Fehsenfeld F, Calvert J, Fall R, Goldan P, Guenther AB, Newitt CN, et al. Emissions of volatile organic compounds from vegetation and the implications for atmospheric chemistry. Glob Biogeochem Cycles 1992;6(4):389–430.

Fiore AM, Horowitz LW, Purves DW, Levy II H, Evans MJ, Wang Y, et al. Evaluating the contribution of changes in isoprene emissions to surface ozone trends over the eastern United States. J Geophys Res 2005;110:D12303, doi:10.1029/2004JD005485.

Geron C, Owen S, Guenther A, Greenberg J, Rasmussen R, Bai J, et al. Volatile organic compounds from vegetation in southern Yunnan Province, China: emission rates and some potential regional implications. Atmos Environ 2006;40:1759–73.

Guenther A, Zimmerman P, Harley P, Monson R, Fall R. Isoprene and monoterpene emission rate variability: model evaluation and sensitivity analysis. J Geophys Res 1993;98:12609–17.

Guenther A, Zimmerman P, Wildermuth M. Natural volatile organic-compound emission rate estimates for United-States woodland landscapes. Atmos Environ 1994;28(6):1197–210.

Guenther A, Hewitt CN, Erickson D, Fall R, Geron C, Graedel T, et al. A global model of natural volatile organic compound emissions. J Geophys Res 1995;100:8873–92.

Guenther A, Geron C, Pierce T, Lamb B, Harley P, Fall R. Natural emissions of non-methane volatile organic compounds, carbon monoxide, and oxides of nitrogen from North America. Atmos Environ 2000;34:2205–30.

He NP, Han XG, Sun W, Pang QM. Biogenic VOC emission inventory development of temperate grassland vegetation in Xilin River Basin, Inner Mongolia China. J Environ Sci (China) 2004;16: 1024–32.

IEA. International Energy Agency, Key World Energy Statistics; 2004.

Klinger LF, Zimmerman P, Greenberg J, Heidt L, Guenther A. Carbon trace gas fluxes along a successional gradient in the Hudson Bay. J Geophys Res 1994;99:1469–94.

Klinger L, Li Q, Guenther A, Greenberg J, Baker B, Bai J. Volatile organic compound emissions related to ecosystem development in China. J Geophys Res 2002;107(D21):4603, doi:10.1029/2001JD001076.

Lack D, Tie X, Neville A, Bofinger D, Wiegand N, Aumont B, et al. Seasonal variability of atmospheric oxidants due to the formation of secondary organic aerosol: a global modeling study. J Geophys Res 2003;108, doi:10.1029/2003JD003418.

Pierce TE, Novak JH. Estimating natural emissions for EPA's regional oxidant model. paper presented at *EPA/AWMA International Speciality Conference* on Emissions Inventory Issues in the 1990s, Environ. Prot. Agency; 1991. Sept. 9–14.

Ryerson TB, Trainer M, Holloway JS, Parrish DD, Huey LG, Super DT, et al. Observations of O_3 formation in power plant plumes and implications for O_3 control strategies. Science 2001;292 (5517):719–23.

Schindlbacher A, Zechmeister-Boltenstern S, Butterbach-Bahl K. Effects of soil moisture and temperature on NO, NO_2 and N_2O emissions from forest soils. J Geophys Res 2004;109(D17302):17302–9.

Schoenemeyer T, Richter K, Smiatek G. Vorstudie uber ein raumlich und zeitlich aufgelostes Kataster anthro-pogener und biogener Emissionen fuer Bayern mit En-twicklung eines PrototYps und Anwendung fur Immissionsprognosen. Abschluss bericht an das Bayerische Landesamt fur Umweltschutz. Fraunhofer-Institut fuer Atmosphaerische Umweltforschung; 1997. Garmisch-Partenkirchen.

Sillman S. The use of NO_y, H_2O_2, and HNO_3 as indicators for ozone-NOx-hydrocarbon sensitivity in urban locations. J Geophys Res 1995;100:14175–88.

Simpson D, Perrin DA, Varey JE, Williams ML. Dispersion modelling of nitrogen oxides in the United Kingdom. Atmos Environ 1990;24A(7):1713–33.

Skiba U, Hargreaves KJ, Fowler D, Smith KA. Fluxes of nitric and nitrous oxide from agricultural soils in a cool temperate climate. Atmos Environ 1992;26..4(14):2477–88.

Stocker DW, Stedman DH, Zeller KF, Massman WJ, Fox DG. Fluxes of nitrogen oxides and ozone measured by eddy correlation over a shortgrass prairie. J Geophys Res 1993;98(12):12,619–30.

Streets DG, Bond TC, Carmichael GR, Fernandes SD, Fu Q, He D, et al. An inventory of gaseous and primary aerosol emissions in Asia in the year 2000. J Geophys Res 2003;108:8809, doi:10.1029/2002JD003093.

Tie X, Brasseur G, Zhao C, Granier C, Massie S, Qin Y, Wang PC, Wang GL, Yang PC. Chemical characterization of air pollution in Eastern China and the Eastern United States. Atmos Environ 2006;40:2607–25.

Wang ZH, Bai YH, Zhang SY. A biogenic volatile organic compound emission inventory for Yunan province. J Environ Sci (China) 2005a;17:353–9.

Wang X, Mauzerall DL, Hu Y, Russell A, Larson E, Woo J, et al. A high-resolution emission inventory for eastern China: 2000 and three 2020 scenarios. Atmos Environd 2005b;39:5917–33.

Wiedinmyer C, Tie X, Guenther A. Changes in biogenic volatile organic emissions that occur as a result of land cover change: How do they affect regional and global atmospheric chemistry? Earth Interact 2006;10:1-19.

Williams E, Fehsenfeld F. Measurement of soil nitrogen oxide emissions at three North American ecosystems. J Geophys Res 1991;96:1033.

Zhang R, Lei W, Tie X, Hess P. Industrial emissions cause extreme diurnal urban ozone variability. Proc Natl Acad Sci U S A 2004;101:6346–50.

Zhao CS, Tie X, Wang GL, Qin Y, Yang PC. Analysis of Air Quality in Eastern China and its Interaction with Other Regions of the World, J. Atmos. Chem. in press.

Zimmerman PR, Greenberg JP, Westberg CE. Measurements of atmospheric hydrocarbons and biogenic emission fluxes in the Amazon boundary-layer. J Geophys Res 1988;93(D2):1407–16.